Relative Orientation of Quadrupole Tensors from High-Resolution NMR of Powdered Solids

Nicholas G. Dowell, Sharon E. Ashbrook, and Stephen Wimperis*

School of Chemistry, University of Exeter, Stocker Road, Exeter EX4 4QD, U.K.

Received: May 30, 2002; In Final Form: July 18, 2002

Techniques such as dynamic-angle spinning (DAS), double rotation (DOR), multiple-quantum MAS (MQMAS), and satellite-transition MAS (STMAS) may be used to obtain high-resolution NMR spectra of half-integer quadrupolar nuclei in powdered solids. These methods enable resolution of crystallographically inequivalent nuclei and also yield the quadrupolar coupling constant C_Q, quadrupolar asymmetry η, and isotropic chemical shift δ_{CS} of each crystallographic site. However, no information is obtained that relates one quadrupole tensor to another, such as internuclear distances or relative orientations. Here, we discuss a recently developed modification of the MQMAS NMR experiment that utilizes two-dimensional correlation of second-order (rank $l = 4$) broadened MAS line shapes to obtain the relative orientation of quadrupole tensors. This new method involves the insertion of a "mixing time", τ_m, into the MQMAS experiment such that magnetization transfer between two distinct nuclei within a crystallite during this period will result in a two-dimensional "cross-peak" correlating the two line shapes. The shapes of these cross-peaks are characteristic of the three Euler angles, α', β', and γ', that describe the relative orientation of the two quadrupole tensors. In this work we use the example of ^{23}Na ($I = {}^3/_2$) NMR of borax ($Na_2B_4O_7 \cdot 10H_2O$) to discuss in more detail the nature of the magnetization transfer. We also derive an analytical expression for the rank $l = 4$ orientational dependence of the second-order quadrupolar interaction in terms of the relative orientation of two quadrupole tensors and simulate the effect upon the shape of the cross-peak when the angles α', β', and γ' are changed. Finally, the use of this novel technique is demonstrated in a ^{23}Na NMR study of sodium metasilicate pentahydrate ($Na_2SiO_3 \cdot 5H_2O$) and in a comparative ^{23}Na NMR study of sodium tungstate dihydrate ($Na_2WO_4 \cdot 2H_2O$) and sodium molybdate dihydrate ($Na_2MoO_4 \cdot 2H_2O$).

Introduction

Extraction of detailed information from solid-state NMR spectra of nuclei with spin quantum number $I > {}^1/_2$, such as ^{11}B and ^{23}Na ($I = {}^3/_2$) and ^{17}O and ^{27}Al ($I = {}^5/_2$), is often hindered by the presence of a significant anisotropic broadening arising from the interaction of the nuclear quadrupole moment eQ with the surrounding electric field gradient tensor **V**.[1] This quadrupolar interaction is usually parametrized by a coupling constant $C_Q = eQV_{z,z}/h$ and an asymmetry $\eta = (V_{x,x} - V_{y,y})/V_{z,z}$, where the $V_{i,i}$ are the principal axes of **V**.[1] The magnitude of this interaction is often such that, for quadrupolar nuclei with half-integer spin, only the central transition ($m_I = +{}^1/_2 \leftrightarrow -{}^1/_2$) is observed by conventional NMR techniques, as this is not broadened by the first-order effects of the quadrupolar interaction. This transition is, however, broadened by a second-order quadrupolar interaction, resulting in inherently low resolution and little potential for yielding useful information if more than one crystallographic site is present. Although magic angle spinning (MAS),[2] rapidly rotating the powder sample around an axis inclined at 54.736° to the external magnetic field, may be employed to reduce the second-order quadrupolar broadening, it is unable to remove it fully and more sophisticated techniques are required.[3] Methods such as dynamic-angle spinning (DAS),[4] double rotation (DOR),[5] multiple-quantum MAS (MQMAS)[6], and most recently, satellite-transition MAS (STMAS)[7] have been successfully used to obtain high-resolution or "isotropic" NMR spectra of quadrupolar nuclei in a wide range of systems.

Recently, in a preliminary communication,[8] we have presented a two-dimensional technique based on the MQMAS experiment of Frydman and Harwood[6] that allows the relative orientation of two quadrupole tensors to be determined. MQMAS removes the second-order quadrupolar broadening via correlation of multiple- and single-quantum coherences under MAS conditions, thereby refocusing the anisotropic quadrupolar broadening, while retaining isotropic shifts.[6,9−13] A two-dimensional Fourier transform yields a spectrum containing "ridge" line shapes that lie along a gradient equal to the ratio of the residual second-order broadenings in the multiple- and single-quantum dimensions (the so-called "MQMAS ratio"), e.g., $-{}^7/_9$ in a spin $I = {}^3/_2$ triple-quantum MAS spectrum. The isotropic spectrum may be obtained from a projection orthogonal to this axis. We have shown that the MQMAS experiment may be readily adapted to provide information on the relative orientation of quadrupole tensors through the insertion of a "mixing time", τ_m,[8] in a manner similar to previous single-quantum correlation techniques.[14,15] Thus, any magnetization transfer during this mixing time between two distinct nuclei within a crystallite will result in "cross-peaks" in the two-dimensional spectrum that correlate the two ridge line shapes.[14,15] The shape of these cross-peaks will be characteristic of the three

* To whom correspondence should be addressed. Fax: +44-1392-263434. E-mail: s.wimperis@exeter.ac.uk.

10.1021/jp021315z CCC: $22.00
Published on Web 09/24/2002

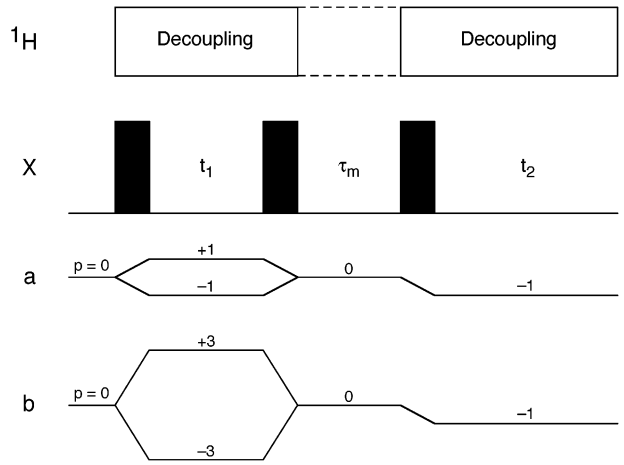

Figure 1. Pulse sequence and coherence transfer pathways for the (a) single-quantum "NOESY-type" correlation experiment and (b) triple-quantum MAS correlation experiment. Magnetization transfer occurs during the mixing time, τ_m, when only population states (coherence order $p = 0$) are retained by the phase cycle. High-power ^{1}H decoupling is normally applied during the t_1 and t_2 periods but may be turned off during τ_m to enhance the spin-diffusion rate.

angles, α', β', and γ', that describe the relative orientation of the two quadrupole tensors.

In this work we describe in more detail the theoretical and experimental aspects of this novel MQMAS correlation experiment. First, we use the example of ^{23}Na NMR of borax to discuss the mechanism of magnetization transfer in experiments on both static and spinning samples. Second, we derive an analytical expression for the orientational dependence of the second-order quadrupolar interaction in terms of the relative orientation of two quadrupole tensors and simulate the effect upon the shape of the cross-peaks obtained in both single- and triple-quantum MAS correlation spectra when the angles α', β' and γ' are changed. Finally, we show further experimental ^{23}Na NMR examples of the use of this technique for determining the relative orientation of quadrupole tensors.

Experimental Section

All NMR experiments were performed on a Bruker MSL/Avance 400 spectrometer, equipped with a widebore 9.4 T magnet, operating at a Larmor frequency of 105.8 MHz for ^{23}Na. Powdered samples were packed inside 4-mm rotors for both static and MAS experiments. Pulses were applied with a radio frequency field strength, $\omega_1(^{23}\text{Na})/2\pi$, of ~100 kHz, except where otherwise stated. When required, ^{1}H decoupling was employed using radio frequency field strengths, $\omega_1(^1\text{H})/2\pi$, between 75 and 100 kHz. Chemical shifts are reported in ppm relative to an external standard of 0.15 M NaCl (aq).

Magnetization Transfer

The pulse sequence for the well-known two-dimensional single-quantum (or "NOESY-type") correlation experiment is shown in Figure 1a.[16,17] During the interval between the final two pulses, or mixing time, τ_m, magnetization is stored along the rotating-frame z axis as an incoherent population state. Figure 2a shows a two-dimensional ^{23}Na NOESY-type spectrum of a static (i.e., nonrotating) sample of borax ($Na_2B_4O_7 \cdot 10H_2O$), recorded with $\tau_m = 0$. Although borax possesses two Na sites that are crystallographically inequivalent,[18] the two do not yield resolved resonances owing to the presence of second-order quadrupolar broadening and, presumably, additional broadening resulting from dipolar or anisotropic chemical shift interactions.

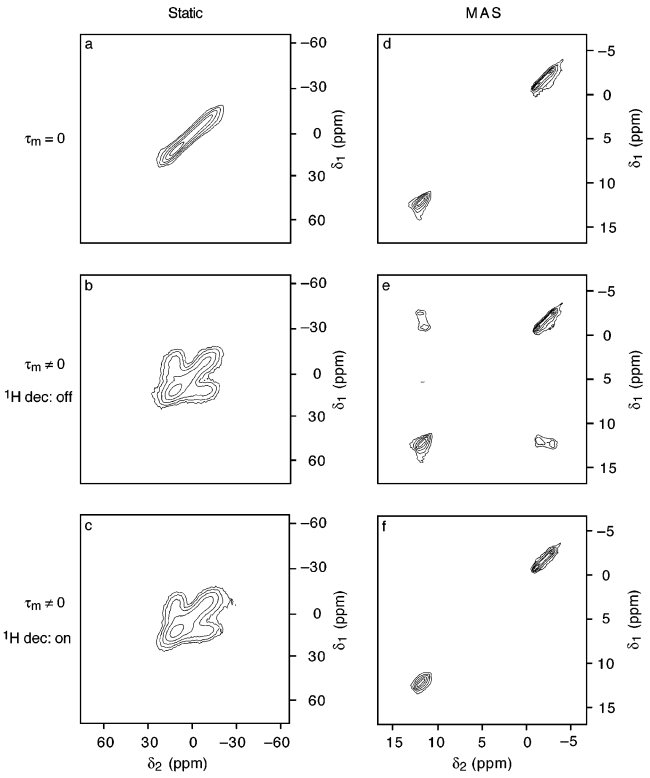

Figure 2. Two-dimensional single-quantum ^{23}Na NMR spectra of borax ($Na_2B_4O_7 \cdot 10H_2O$), recorded with the sample static (a−c) and spinning at the magic angle (d−f). Mixing times: (a) $\tau_m = 0$; (b) $\tau_m =$ 100 ms with no ^{1}H decoupling; (c) $\tau_m = 100$ ms with ^{1}H decoupling; (d) $\tau_m = 0$; (e) $\tau_m = 75$ ms with no ^{1}H decoupling; and (f) $\tau_m = 75$ ms with ^{1}H decoupling. The spectra were recorded using the pulse sequence shown in Figure 1a with (a−c) 24 transients averaged for each of 128 t_1 increments of 16.67 μs and with (d−f) 8 transients averaged for each of 256 t_1 increments of 100 μs. The recycle interval between transients was (a−c) 2 s and (d−f) 2.5 s. The MAS rate in (d−f) was 4.0 kHz.

The spectrum, therefore, consists of a single, continuous ridge along the $\delta_1 = \delta_2$ autocorrelation "diagonal".

If the mixing time is nonzero, magnetization may be transferred between the two distinct Na sites in borax via a "spin diffusion" process driven by dipolar interactions connecting the ^{23}Na spins.[19,20] Figure 2b shows the ^{23}Na NOESY-type spectrum of a static borax sample recorded with a mixing time, $\tau_m =$ 100 ms, during which no ^{1}H decoupling was applied. Dipolar-driven magnetization transfer has resulted in significant cross-peak (off-diagonal) intensity in addition to the diagonal ridge. Owing to the low spectral resolution, these cross-peaks are broad and overlap both with each other and with the diagonal ridge. The presence of a strongly coupled network of ^{1}H spins often significantly enhances the magnetization transfer rate ("^{1}H-driven spin diffusion"[20]) by broadening the energy levels of the observed nucleus. However, in Figure 2c, where ^{1}H decoupling was applied throughout a mixing time $\tau_m = 100$ ms, cross-peaks are still observed, indicating that in static samples of borax the presence of ^{1}H nuclei is not required for ^{23}Na−^{23}Na spin diffusion to proceed.

Resolution in NMR of solids may be increased through the use of MAS,[2] where the powder sample is rotated around an axis inclined at an angle of 54.736° to the static magnetic field. This averages the first-order quadrupolar broadening and the rank $l = 2$ component of the second-order quadrupolar broadening to zero, but is not able to remove the rank $l = 4$ component of the second-order interaction fully.[3] Broadenings resulting from chemical shift anisotropy and inhomogeneous dipolar

interactions will be removed, although homogeneous dipolar couplings will not be suppressed unless the MAS rate is sufficiently fast.

Figure 2d shows a two-dimensional ^{23}Na MAS NMR NOESY-type spectrum of borax, recorded with $\tau_m = 0$. The two inequivalent Na sites give rise to ^{23}Na resonances that are now fully resolved under MAS, both lying along the $\delta_1 = \delta_2$ diagonal. The inclusion of a mixing time, $\tau_m = 75$ ms with no ^{1}H decoupling, results in two off-diagonal cross-peaks that correlate the two ^{23}Na line shapes, as shown in Figure 2e. As a result of the MAS line-narrowing, these cross-peaks are now also well resolved, both from the diagonal peaks and from each other, allowing for more detailed analysis. The appearance of cross-peaks confirms that in this sample the dipolar-driven ^{23}Na−^{23}Na magnetization transfer is not suppressed by MAS, probably as a consequence of both the relatively slow MAS rate (~4 kHz) employed and the presence of a strongly coupled network of ^{1}H nuclei.[17] This last point is confirmed in Figure 2f, which shows the ^{23}Na MAS NOESY-type spectrum recorded with a mixing time of 75 ms during which ^{1}H decoupling was applied. This spectrum consists only of the two ^{23}Na resonances on the diagonal, with no evidence of off-diagonal cross-peaks. Thus, it appears that MAS is here fully suppressing the homonuclear ^{23}Na−^{23}Na dipolar interaction but that, as long as ^{1}H decoupling is not applied, it is insufficiently fast to suppress the ^{1}H-driven spin diffusion.

Recently, techniques have begun to appear that allow "recoupling" of the homonuclear dipolar interaction between quadrupolar nuclei under MAS conditions.[21−23] Although still at an early developmental stage, such methods are promising as they could be used to increase the rate of magnetization transfer between quadrupolar nuclei in MAS experiments, thereby permitting the study of a wider range of materials, including those not containing abundant high-γ nuclei such as ^{1}H or ^{19}F.

MQMAS Correlation Experiment

The two-dimensional MAS NMR spectra of borax in Figure 2d−f show the highly unusual case of two distinct ^{23}Na resonances fully resolved by an isotropic chemical shift difference. In the vast majority of multisite compounds the conventional MAS NMR spectrum consists of unresolved second-order broadened line shapes. Thus, a two-dimensional NOESY-type spectrum contains cross-peaks that overlap with the diagonal ridge and with each other, potentially obscuring any orientational information contained within the detailed cross-peak structure. In such cases, the resolution may be improved through use of a multiple-quantum (MQ) approach,[6] as shown by the pulse sequence in Figure 1b. Here, triple-quantum coherences, selected by phase cycling,[24] are correlated with single-quantum coherences under MAS conditions in an MQMAS experiment.[6] The pulse sequence is similar to the *z*-filter sequence of Amoureux et al.,[25] except that the interval between the final two pulses, normally of negligible duration, has been extended to become a mixing time, τ_m, during which magnetization transfer can take place. As with many MQMAS experiments, the final pulse has a much-reduced amplitude, acting selectively on the central transition.[12,25] As the spectrum is recorded under MAS conditions, ^{1}H decoupling is not applied during the mixing time, allowing magnetization transfer to be enhanced by any abundant ^{1}H nuclei in the sample. Decoupling may still be employed in the t_1 and t_2 periods, however, to increase the spectral resolution.

The conventional two-dimensional triple-quantum ^{23}Na MAS NMR spectrum of borax, recorded with a *z*-filtered pulse sequence,[25] is shown in Figure 3a. The spectrum consists of two ridge line shapes lying along a gradient of $-7/9$.[6] A cross-section along each ridge line shape still contains the anisotropic second-order quadrupolar broadening, allowing extraction of the quadrupolar parameters C_Q and η. The high-resolution spectrum, obtained from a projection onto an axis orthogonal to the $-7/9$ gradient, consists of two sharp peaks corresponding to the two crystallographically inequivalent Na sites in borax. If a mixing time of 100 ms is included (with no ^{1}H decoupling), two cross-peaks appear that correlate the two MQMAS line shapes, as shown in Figure 3b. In most cases, the higher resolution offered by the MQMAS technique will be crucial in obtaining well-resolved cross-peaks that can be analyzed to yield the relative orientation of the quadrupole tensors.

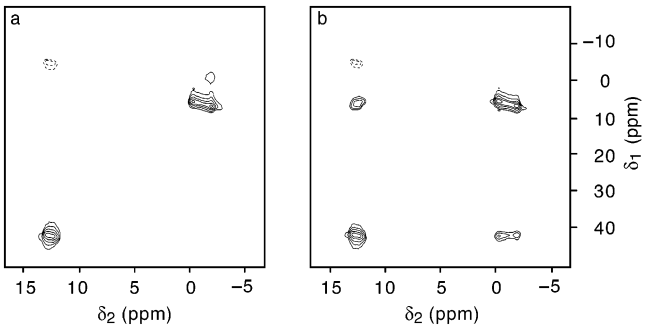

Figure 3. Two-dimensional triple-quantum ^{23}Na MAS NMR spectra of borax with (a) $\tau_m = 0$ and (b) $\tau_m = 100$ ms with no ^{1}H decoupling. The spectra were recorded using the pulse sequence in Figure 1b with 24 transients averaged for each of 512 t_1 increments of 16.67 μs. The recycle interval between transients was 2.5 s, and the MAS rate was 9.0 kHz.

Relative Tensor Orientation and Second-Order Quadrupolar Broadening

A crystallographically distinct nucleus, *k*, possesses a quadrupole tensor $\mathbf{Q}_k = eQ\mathbf{V}_k/2I(2I-1)\hbar$. The two-dimensional NMR experiments described above involve magnetization transfer between two distinct nuclei with different quadrupole tensors, $\mathbf{Q}_1$ and $\mathbf{Q}_2$, during a mixing time τ_m. In the two-dimensional spectrum this results in two cross-peaks which cross-correlate the MAS line shapes.[14−16] Each cross-peak is the sum of homogeneous resonances whose frequency in one dimension depends on the angles β_1 and γ_1 that describe the orientation of $\mathbf{Q}_1$ relative to a rotor-fixed axis system and, in the other dimension, upon the angles β_2 and γ_2 that describe the orientation of $\mathbf{Q}_2$. Overall, the shape of the cross-peak will depend on the three Euler angles, α', β', and γ', that define the relative orientation of the two quadrupole tensors.

For a static sample, the frequencies of the central ($m_I = {}^1/_2$) and triple-quantum ($m_I = {}^3/_2$) transitions subject to a second-order quadrupolar interaction are given by[12,26]

$$\omega^{(2)}_{m_I \leftrightarrow -m_I} = \frac{(\omega_Q^{PAS})^2}{\omega_0}\{A^0(I,m_I)Q^0(\eta) + A^2(I,m_I)Q^2(\xi,\theta,\phi,\eta) + A^4(I,m_I)Q^4(\xi,\theta,\phi,\eta)\} \quad (1)$$

where the $A^l(I,m_I)$ are rank-, spin-, and transition-dependent coefficients,[12] ω_0 is the Larmor frequency, ω_Q^{PAS} is a quadrupolar parameter related to C_Q,

$$\omega_Q^{PAS}/2\pi = \frac{3C_Q}{4I(2I-1)} \quad (2)$$

and where the orientation- and η-dependent Q^l factors are given by

$$Q^0(\eta) = \left(1 + \frac{\eta^2}{3}\right) \tag{3a}$$

$$Q^2(\xi,\theta,\phi,\eta) = \left(1 - \frac{\eta^2}{3}\right) D^2_{0,0}(\xi,\theta,\phi) - \frac{\sqrt{2}}{\sqrt{3}}\eta\{D^2_{0,2}(\xi,\theta,\phi) + D^2_{0,-2}(\xi,\theta,\phi)\} \tag{3b}$$

$$Q^4(\xi,\theta,\phi,\eta) = \left(1 + \frac{\eta^2}{18}\right) D^4_{0,0}(\xi,\theta,\phi) + \frac{\sqrt{10}}{6}\eta\{D^4_{0,2}(\xi,\theta,\phi) + D^4_{0,-2}(\xi,\theta,\phi)\} + \frac{35}{18\sqrt{70}}\eta^2\{D^4_{0,4}(\xi,\theta,\phi) + D^4_{0,-4}(\xi,\theta,\phi)\} \tag{3c}$$

The $D^l_{p',p}(\xi,\theta,\phi)$ are Wigner rotation matrix elements of rank l.[27,28] The three Euler angles, ξ, θ, and ϕ, describe the rotation of the quadrupole tensor from its principal axis system (PAS) into the laboratory frame.

The rank $l = 2$ anisotropic term in eq 1, $Q^2(\xi,\theta,\phi,\eta)$, will average to zero under MAS conditions. Hence, the MAS-averaged second-order frequencies can be written

$$\langle\omega^{(2)}_{m_I\leftrightarrow -m_I}\rangle = \frac{(\omega_Q^{PAS})^2}{\omega_0}\{A^0(I,m_I)Q^0(\eta) + A^4(I,m_I)\langle Q^4(\xi,\theta,\phi,\eta)\rangle\} \tag{4}$$

where the angle brackets $\langle\ \rangle$ indicate averaging by MAS.

For a spinning sample, the transformation from the PAS of the quadrupole tensor $\mathbf{Q}_1$ to the laboratory frame is broken down into two stages, with transformation via an intermediate rotor-fixed axis system. From eq 4, the effect of such an extra transformation need only be considered for the rank $l = 4$ orientational factor $Q^4(\xi,\theta,\phi,\eta)$. If we start by assuming, for simplicity, that the quadrupole tensor is axially symmetric, $\eta_1 = 0$, then, under spinning conditions, the rank $l = 4$ factor can be expanded as follows:[27,28]

$$Q^4(\xi_1,\theta_1,\phi_1,\eta_1{=}0) = D^4_{0,0}(\xi_1,\theta_1,\phi_1) = \sum_m D^4_{0,m}(0,\chi,\omega_R t) D^4_{m,0}(\alpha_1,\beta_1,0) \tag{5}$$

where ω_R is the MAS frequency and α_1, β_1 are the two Euler angles describing the rotation from the $\mathbf{Q}_1$ PAS to the rotor-fixed axis system. If an average over one rotor period is now taken then only terms with $m = 0$ will be retained, yielding,

$$\langle Q^4(\xi_1,\theta_1,\phi_1,\eta_1{=}0)\rangle = d^4_{0,0}(\chi)d^4_{0,0}(\beta_1) \tag{6}$$

where χ is the angle of the rotor axis with respect to the static magnetic field B_0, i.e., 54.736° for MAS. In this case, only the angle β_1 is needed to describe the orientation of the unique axis of the $\eta_1 = 0$ quadrupole tensor with respect to this spinning axis.

However, if a two-dimensional correlation spectrum is to be calculated, the second quadrupole tensor $\mathbf{Q}_2$ must be transformed from its PAS into the $\mathbf{Q}_1$ PAS before being transformed into the rotor frame and finally into the laboratory frame. This ensures that the orientation of the second quadrupole tensor is now expressed relative to that of the first. If we assume that the second tensor also has $\eta_2 = 0$ then the expansion of the rank $l = 4$ orientational factor becomes

$$Q^4(\xi_2,\theta_2,\phi_2,\eta_2{=}0) = \sum_m\sum_n D^4_{0,m}(0,\chi,\omega_R t)\, D^4_{m,n}(\alpha_1,\beta_1,\gamma_1)D^4_{n,0}(\alpha',\beta',0) \tag{7}$$

where α', β' are the two Euler angles describing the rotation from the second quadrupole tensor PAS to the first. As shown previously, only the terms with $m = 0$ are nonzero if an average over one rotor period is taken,

$$\begin{aligned}\langle Q^4(\xi_2,\theta_2,\phi_2,\eta_2{=}0)\rangle &= d^4_{0,0}(\chi)\sum_n D^4_{0,n}(0,\beta_1,\gamma_1)D^4_{n,0}(\alpha',\beta',0)\\ &= d^4_{0,0}(\chi)[d^4_{0,0}(\beta_1)d^4_{0,0}(\beta') - 2d^4_{1,0}(\beta_1)d^4_{1,0}(\beta')\cos(\alpha'+\gamma_1) + 2d^4_{2,0}(\beta_1)d^4_{2,0}(\beta')\cos2(\alpha'+\gamma_1) - 2d^4_{3,0}(\beta_1)d^4_{3,0}(\beta')\cos3(\alpha'+\gamma_1) + 2d^4_{4,0}(\beta_1)d^4_{4,0}(\beta')\cos4(\alpha'+\gamma_1)]\end{aligned} \tag{8}$$

Here, β' is the single fixed angle that describes the relative orientation of the two quadrupole tensors when both tensors are axially symmetric, i.e., $\eta_1 = \eta_2 = 0$.[8] The angle α' can be neglected as it always occurs in eq 8 as $(\alpha' + \gamma_1)$, which will be averaged from 0 to 2π in a powder sample, while it is absent from eq 6.

The expressions in eqs 4, 6, and 8 may be used for frequency-domain computer simulation of two-dimensional correlation spectra. The simulation is performed by looping over a large number (~100 000) of evenly distributed values of the angles β_1 and γ_1, with a fixed angle, β', describing the relative orientation of two quadrupole tensors of magnitudes C_{Q_1} and C_{Q_2}, with $\eta_1 = \eta_2 = 0$. An isotropic chemical shift is also included for each distinct nucleus considered. For each pair of β_1 and γ_1 angles, the frequencies in the δ_1 and δ_2 dimensions of the spectrum are calculated. For the two diagonal peaks these frequencies are calculated via either eq 6 or eq 8 in both dimensions, whereas the cross-peaks arise from frequencies which are calculated via eq 6 in one dimension and eq 8 in the other. The spectrum is then constructed in the form of a two-dimensional histogram with each addition to the histogram weighted by a $\sin\beta_1$ spherical averaging factor.[8]

The expressions for the central and triple-quantum transition frequencies become more complex when axial symmetry is not assumed, but the procedure outlined above is not significantly altered. If $\eta \neq 0$ then the MAS-averaged rank $l = 4$ orientational factor becomes[12,26]

$$\langle Q^4(\xi,\theta,\phi,\eta)\rangle = \left(1 + \frac{\eta^2}{18}\right)\langle D^4_{0,0}(\xi,\theta,\phi)\rangle + \frac{\sqrt{10}}{6}\eta\{\langle D^4_{0,2}(\xi,\theta,\phi)\rangle + \langle D^4_{0,-2}(\xi,\theta,\phi)\rangle\} + \frac{35}{18\sqrt{70}}\eta^2\{\langle D^4_{0,4}(\xi,\theta,\phi)\rangle + \langle D^4_{0,-4}(\xi,\theta,\phi)\rangle\} \tag{9}$$

It is clear the additional transformation via the rotor frame now necessitates expansion of Wigner rotation matrix elements of the form $D^4_{0,p}(\xi,\theta,\phi)$, where $p = 0$, ±2, and ±4. Considering the first quadrupole tensor $\mathbf{Q}_1$, therefore, this expansion can be expressed as

$$D^4_{0,p}(\xi_1,\theta_1,\phi_1) = \sum_m D^4_{0,m}(0,\chi,\omega_R t)D^4_{m,p}(\alpha_1,\beta_1,\gamma_1) \tag{10}$$

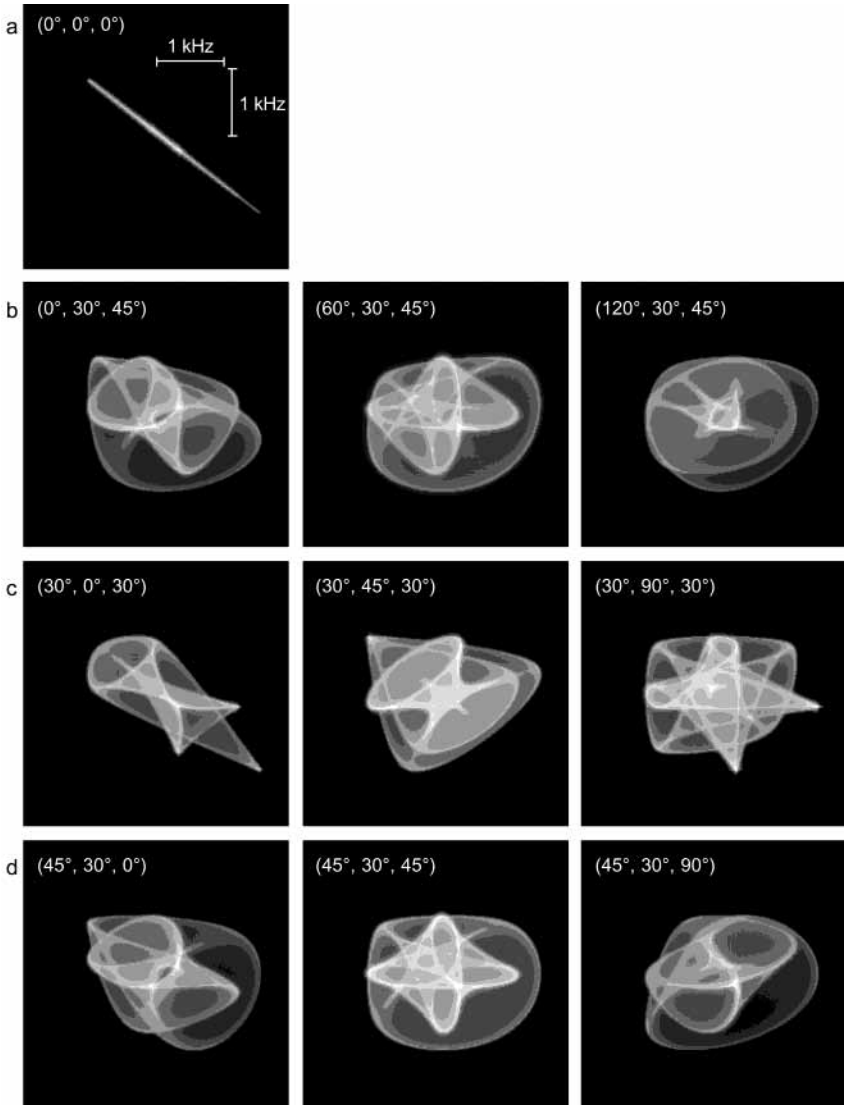

Figure 4. Computer-simulated triple-quantum MAS NMR correlation spectra for two spin I = 3/2 nuclei. Only the high-field cross-peak is shown. In (a) both quadrupole tensors are collinear, i.e., Euler angles (α', β', γ') = (0°, 0°, 0°). Cross-peaks in (b−d) show the effect of changing α', β' and γ', respectively. Simulation parameters: $C_{Q_1} = C_{Q_2} = 2.0$ MHz; $\eta_1 = \eta_2 = 0.7$; $\omega_0/2\pi = 105.8$ MHz; $\delta_{CS_1} - \delta_{CS_2} = 40$ ppm; and 20 Hz Lorentzian linebroadening (full-width at half-height).

On averaging over a rotor period, one obtains

$$\langle D^4_{0,p}(\xi_1,\theta_1,\phi_1)\rangle = d^4_{0,0}(\chi)D^4_{0,p}(0,\beta_1,\gamma_1) = d^4_{0,0}(\chi)d^4_{0,p}(\beta_1)e^{-ip\gamma_1} \quad (11)$$

It should be noted that two angles, β_1 and γ_1, are now needed to describe the orientation of the tensor in the rotor frame and also that, when $p = 0$, this expression reduces to that given in eq 6.

For the second quadrupole tensor $\mathbf{Q}_2$, again an additional initial transformation into the $\mathbf{Q}_1$ PAS must be performed to obtain expressions that involve the relative orientation of the two tensors. The expansion of the Wigner elements becomes

$$D^4_{0,p}(\xi_2,\theta_2,\phi_2) = \sum_m\sum_n D^4_{0,m}(0,\chi,\omega_R t)\, D^4_{m,n}(\alpha_1,\beta_1,\gamma_1)D^4_{n,p}(\alpha',\beta',\gamma') \quad (12)$$

where α', β', and γ' are the three fixed angles that describe the relative orientation of the two tensors. On averaging over a rotor period, only terms with $m = 0$ are retained,

$$\langle D^4_{0,p}(\xi_2,\theta_2,\phi_2)\rangle = d^4_{0,0}(\chi)\sum_n D^4_{0,n}(0,\beta_1,\gamma_1)D^4_{n,p}(\alpha',\beta',\gamma') = d^4_{0,0}(\chi)\sum_n d^4_{0,n}(\beta_1)d^4_{n,p}(\beta')\, e^{-i(n(\alpha'+\gamma_1)+p\gamma')} \quad (13)$$

Note that, when $p = 0$, this expression reduces to that given in eq 8.

Two-dimensional correlation spectra may be simulated as described above, but now using eqs 11 and 13 in conjunction with eqs 4 and 9. In the case where both quadrupole tensors are axially asymmetric, i.e., $\eta_1 \neq 0$ and $\eta_2 \neq 0$, then the calculation is performed with powder averaging over β_1 and γ_1 as described previously, but with three fixed angles, α', β', and γ', describing the relative tensor orientation. All three angles appear in the expression in eq 13 and, although α' always occurs as ($\alpha' + \gamma_1$), the angle γ_1 appears in eq 11 while α' does not, with the result that in a correlation simulation the value of α' cannot be ignored. However, for the case where the asymmetry

of only one of the quadrupole tensors is nonzero, e.g., $\eta_1 = 0$ but $\eta_2 \neq 0$, the two frequencies correlated in the cross-peaks now involve the expressions in eq 6 and eq 13. The angle γ_1 does not appear in eq 6 with the result that the value of α' is irrelevant and the relative orientation of the two tensors in this case is described by only two fixed angles, β' and γ'. Furthermore, it should be noted that, if $\eta_1 \neq 0$ but $\eta_2 = 0$, the cross-peak is simulated via correlation of eq 8 and eq 11 and is again described by only two fixed angles, now α' and β'.

Some cross-peaks from triple-quantum MAS correlation spectra of two spin I = 3/2 nuclei that both have $C_Q = 2.0$ MHz and $\eta = 0.7$ are simulated in Figure 4. As both quadrupole tensors possess nonzero asymmetries their relative orientation is defined by three Euler angles, α', β', and γ'. Figure 4 demonstrates that the shape of the cross-peak is very dependent upon the values of these angles, with significant changes occurring when any one of the three is varied. When all three angles are zero, i.e., when $\mathbf{Q}_1$ and $\mathbf{Q}_2$ share a common PAS, and when η is the same for each tensor, the cross-peak is a sharp ridge line shape (Figure 4a).

In Figure 4 the three Euler angles describing the relative tensor orientation are shown varied over different ranges of values. By definition, α' and γ' lie between 0 and 360°, while β' is defined only between 0 and 180°.[28] However, the symmetry of the expressions described above and the effects of powder averaging limit the meaningful range to $0 \leq \alpha' \leq 180°$ and $0 \leq \beta', \gamma' \leq 90°$, with unique cross-peaks only found between these values. Thus, the cross-peak described by $(180° - \alpha', \beta', \gamma')$ is distinct from the cross-peak described by $(\alpha', \beta', \gamma')$ and both of these are unique shapes within the defined range. However, the cross-peaks described by $(\alpha', 180° - \beta', \gamma')$ or $(\alpha', \beta', 180° - \gamma')$ are identical to that described by $(180° - \alpha', \beta', \gamma')$.

Experimental Results

The theory outlined above has demonstrated that the shape of the cross-peaks obtained in experimental MQMAS correlation spectra may be analyzed to obtain the three angles, α', β', and γ', describing the relative orientation of the quadrupole tensors involved, provided that the quadrupolar parameters C_Q and η, and isotropic chemical shift δ_{CS} of each nucleus, may be accurately determined. The experimental MAS spectra shown so far (^{23}Na NMR of borax in Figures 2d−f and 3) have not necessitated a multiple-quantum approach to resolve the two distinct Na sites and, owing to the two very small C_Q values involved, the cross-peaks obtained in both single- and multiple-quantum correlation spectra do not possess much well-defined structure. However, a previous ^{23}Na NMR single-crystal study of borax has determined the relative orientation of the two tensors[18] and provides a simple test of the method. Figure 5a shows the two-dimensional ^{23}Na MAS NMR NOESY-type spectrum of borax, recorded using the pulse sequence in Figure 1a with a mixing time of 400 ms. Figure 5b shows the corresponding spectrum, simulated with a fixed orientation $(\alpha', \beta', \gamma')$ of (81°, 52°, 40°) between two nuclei, $k = 1$ with $C_{Q_1} = 0.541$ MHz, $\eta_1 = 0.449$ and $\delta_{CS_1} = 11.4$ ppm, and $k = 2$ with $C_{Q_2} = 0.849$ MHz, $\eta_2 = 0.143$, and $\delta_{CS_2} = -1.6$ ppm, with $\omega_0/2\pi = 105.8$ MHz.[18] Despite the lack of much fine structure in the cross-peaks, it can be seen that the simulated spectrum is in good agreement with the experimental spectrum.

Figure 6a shows a two-dimensional triple-quantum ^{23}Na MAS NMR spectrum of sodium metasilicate pentahydrate ($Na_2SiO_3 \cdot 5H_2O$), recorded using a conventional *z*-filter pulse sequence.[25] Two ridge line shapes are observed lying along gradients of

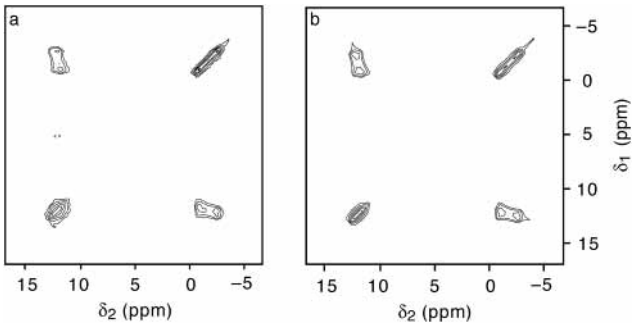

Figure 5. (a) Experimental and (b) computer-simulated two-dimensional single-quantum ^{23}Na MAS NMR spectrum of borax. Experimental parameters in (a): pulse sequence in Figure 1a; 8 transients averaged for 256 t_1 increments of 100 μs; $\tau_m = 400$ ms with no ^{1}H decoupling; 2.5 s recycle interval between transients; and 4.0 kHz MAS rate. Simulation parameters in (b): relative tensor orientation $(\alpha', \beta', \gamma') = (81°, 52°, 40°)$; $C_{Q_1} = 0.541$ MHz; $C_{Q_2} = 0.849$ MHz; $\eta_1 = 0.449$; $\eta_2 = 0.143$; $\delta_{CS_1} = 11.4$ ppm; $\delta_{CS_2} = -1.6$ ppm; $\omega_0/2\pi = 105.8$ MHz; and 26 Hz Lorentzian linebroadening (full-width at half-height).

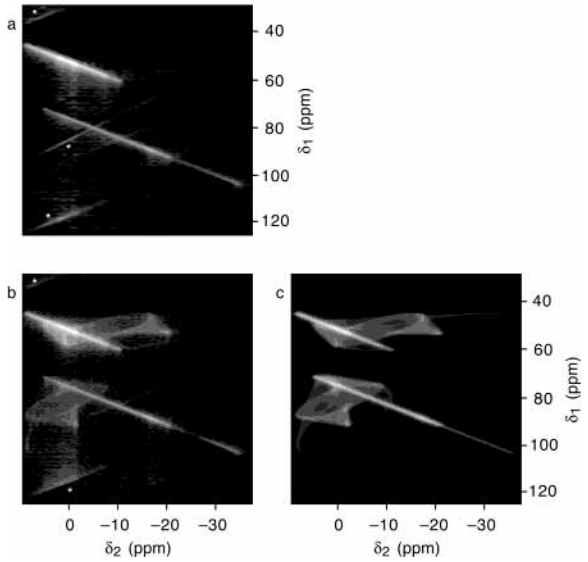

Figure 6. (a, b) Experimental and (c) computer-simulated two-dimensional triple-quantum ^{23}Na MAS NMR spectra of sodium metasilicate pentahydrate ($Na_2SiO_3 \cdot 5H_2O$). Experimental parameters in (a): pulse sequence in Figure 1b; $\tau_m = 0$; 48 transients averaged for 512 t_1 increments of 16.67 μs; 2.0 s recycle interval; and 9.0 kHz MAS rate. Experimental parameters in (b): pulse sequence in Figure 1b; $\tau_m = 400$ ms with no ^{1}H decoupling; 192 transients averaged for 576 t_1 increments of 14.7 μs; 2.0 s recycle interval; and 9.0 kHz MAS rate. Spinning sidebands are denoted by *. Simulation parameters in (c): relative tensor orientation $(\alpha', \beta', \gamma') = (90°, 35°, 10°)$; $C_{Q_1} = 1.8$ MHz; $C_{Q_2} = 2.8$ MHz; $\eta_1 = 0.75$; $\eta_2 = 0.17$; $\delta_{CS_1} = 9.0$ ppm; $\delta_{CS_2} = 9.5$ ppm; $\omega_0/2\pi = 105.8$ MHz; and 60 Hz Lorentzian linebroadening (full-width at half-height).

$-7/9$, corresponding to the two crystallographically inequivalent Na sites in this compound.[29] Other ridges, marked with an asterisk, correspond to spinning sidebands. Cross sections along the ridges reveal anisotropically broadened line shapes corresponding to quadrupolar parameters of $C_{Q_1} = 1.8$ MHz, $\eta_1 = 0.75$, and $C_{Q_2} = 2.8$ MHz, $\eta_2 = 0.17$, and to isotropic chemical shifts of $\delta_{CS_1} = 9.0$ ppm and $\delta_{CS_2} = 9.5$ ppm. The inclusion of a mixing time, $\tau_m = 400$ ms with no ^{1}H decoupling, into the MQMAS experiment, as shown in Figure 1b, results in cross-peaks that cross-correlate the two autocorrelation ridges, as shown in Figure 6b. These cross-peaks, although of low amplitude, show well-defined fine structure and are well separated from each other owing to the increase in resolution

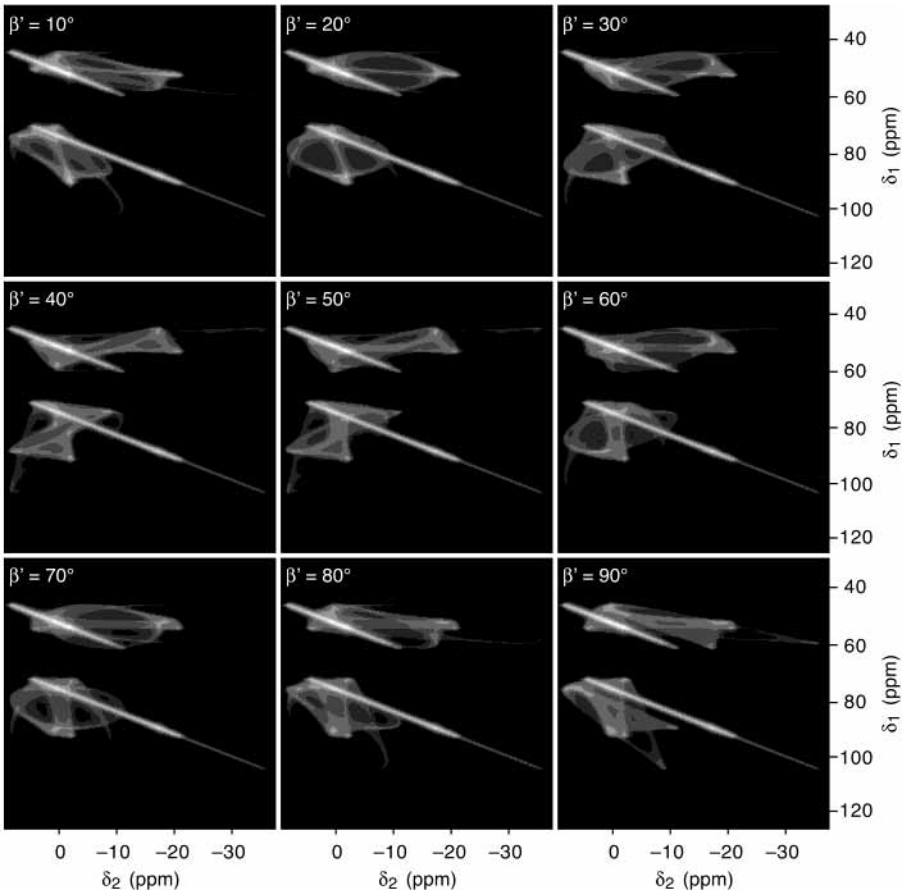

Figure 7. Two-dimensional triple-quantum MAS NMR spectra, simulated using the ^{23}Na parameters for sodium metasilicate pentahydrate ($Na_2SiO_3 \cdot 5H_2O$): $C_{Q_1} = 1.8$ MHz; $C_{Q_2} = 2.8$ MHz; $\eta_1 = 0.75$; $\eta_2 = 0.17$; $\delta_{CS_1} = 9.0$ ppm; $\delta_{CS_2} = 9.5$ ppm; $\omega_0/2\pi = 105.8$ MHz; and 60 Hz Lorentzian linebroadening (full-width at half-height). The Euler angle β' is varied between 10° and 90°, while α' and γ' are 90° and 10°, respectively.

provided by the MQMAS approach,[6] although there is still some overlap with the autocorrelation ridges.

The distinctive shapes of the cross-peaks in Figure 6b are characteristic of the α', β', and γ' angles that define the relative orientation of the two quadrupole tensors. Figure 7 shows triple-quantum correlation spectra, simulated using the ^{23}Na NMR parameters of sodium metasilicate pentahydrate, for 10° increments of the β' angle (for the purposes of illustration, the α' and γ' angles are fixed at 90° and 10°, respectively). Inspection of this figure reveals that the two cross-peaks simulated with $\beta' = 30°$ are most similar to those obtained experimentally. This procedure was repeated in an interactive fashion, cycling through the three Euler angles with ever finer angle increments, until a satisfactory match was obtained with the angles $\alpha' = 90° \pm 10°$, $\beta' = 35° \pm 2°$, and $\gamma' = 10° \pm 5°$. This simulation is shown in Figure 6c.

Although the cross-peaks in a NOESY-type, single-quantum correlation experiment are usually overlapped with each other and with the autocorrelation diagonal, considerable fine structure often remains observable. Figure 8a shows a two-dimensional ^{23}Na NOESY-type spectrum of sodium metasilicate pentahydrate recorded using the pulse sequence in Figure 1a with $\tau_m = 0$. The two inequivalent Na sites are not resolved and the spectrum consists of a single ridge along the autocorrelation diagonal. Figure 8b shows the corresponding spectrum obtained with a mixing time of $\tau_m = 1.0$ s (with no ^{1}H decoupling applied during this period). The spectrum displays well-structured cross-peaks overlapping both each other and the diagonal. The relative orientation of the two quadrupole tensors is difficult to determine from this spectrum alone as the overlapping of the peaks hinders

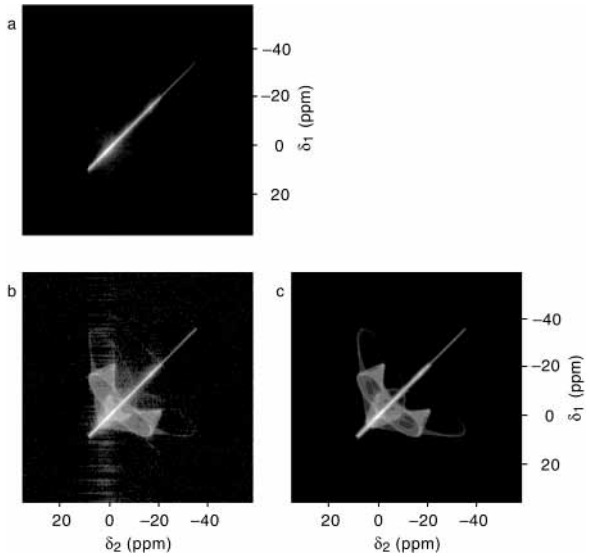

Figure 8. (a, b) Experimental and (c) computer-simulated two-dimensional single-quantum ^{23}Na MAS NMR spectra of sodium metasilicate pentahydrate ($Na_2SiO_3 \cdot 5H_2O$). Experimental parameters in (a, b): pulse sequence in Figure 1a; (a) $\tau_m = 0$ and (b) $\tau_m = 1.0$ s with no ^{1}H decoupling; (a) 8 and (b) 96 transients averaged for 512 t_1 increments of 25 μs; 2.0 s recycle interval; and 9.0 kHz MAS rate. Simulation parameters in (c): same as those in Figure 6c, except 40 Hz Lorentzian linebroadening (full-width at half-height).

detailed analysis. However, it is possible to use such a spectrum as a test of the parameters obtained from the triple-quantum MAS correlation experiment. Figure 8c displays the correspond-

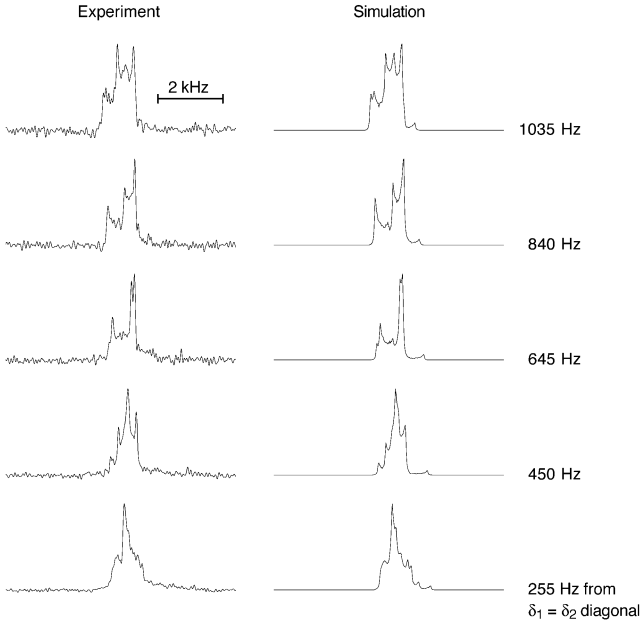

Figure 9. Cross-sections parallel to the $\delta_1 = \delta_2$ diagonal through the experimental and computer-simulated two-dimensional single-quantum ^{23}Na MAS NMR correlation spectra in Figure 8b,c.

ing spectrum simulated with the quadrupolar and chemical shift parameters determined previously and with a relative tensor orientation, (α', β', γ'), of (90°, 35°, 10°) as found above. Good agreement may be seen between this simulated spectrum and the experimental spectrum in Figure 8b, confirming the orientational information obtained from the triple-quantum correlation experiment.

As it is notoriously difficult to compare experimental and simulated contour plots, Figure 9 shows a series of cross-sections extracted parallel to the autocorrelation diagonal in the experimental and simulated spectra in Figures 8b and 8c, respectively. The cross-sections taken from the simulated spectrum display line shapes which are in excellent agreement to those obtained experimentally, providing further confirmation of the accuracy of the angle determination. Although computer-fitting of the full two-dimensional spectrum may be difficult, it could be envisaged that an automated fitting of selected cross-sections may provide an efficient and objective method for the accurate determination of the α', β', and γ' angles.

A further example of the use of the triple-quantum MAS correlation method to obtain the relative orientation of two quadrupole tensors is shown in Figure 10. Figure 10a shows the two-dimensional triple-quantum ^{23}Na MAS NMR spectrum of sodium tungstate dihydrate ($Na_2WO_4 \cdot 2H_2O$). Two resonances are apparent, corresponding to the two crystallographically inequivalent Na sites, with one ridge much longer than the other. The NMR parameters obtained from this spectrum, $C_{Q_1} = 0.88$ MHz, $C_{Q_2} = 2.70$ MHz, $\eta_1 = 0.35$, $\eta_2 = 0.09$, $\delta_{CS_1} = -0.9$ ppm, and $\delta_{CS_2} = 6.3$ ppm, confirm the literature values.[30] Figure 10b shows the two-dimensional spectrum after the inclusion of a mixing time, $\tau_m = 200$ ms with no ^{1}H decoupling, into the experiment, as in Figure 1b. Two cross-peaks appear in this spectrum as a result of dipolar-driven spin diffusion, with that at low-field exhibiting the most structure. An expansion of this cross-peak is shown in Figure 10c. We have not been able to obtain a satisfactory match between this cross-peak and a simulation, despite an extensive search though all possible relative orientations. However, sodium tungstate dihydrate is exactly isostructural with sodium molybdate dihydrate ($Na_2MoO_4 \cdot 2H_2O$),[31] while its NMR parameters are almost identical to those

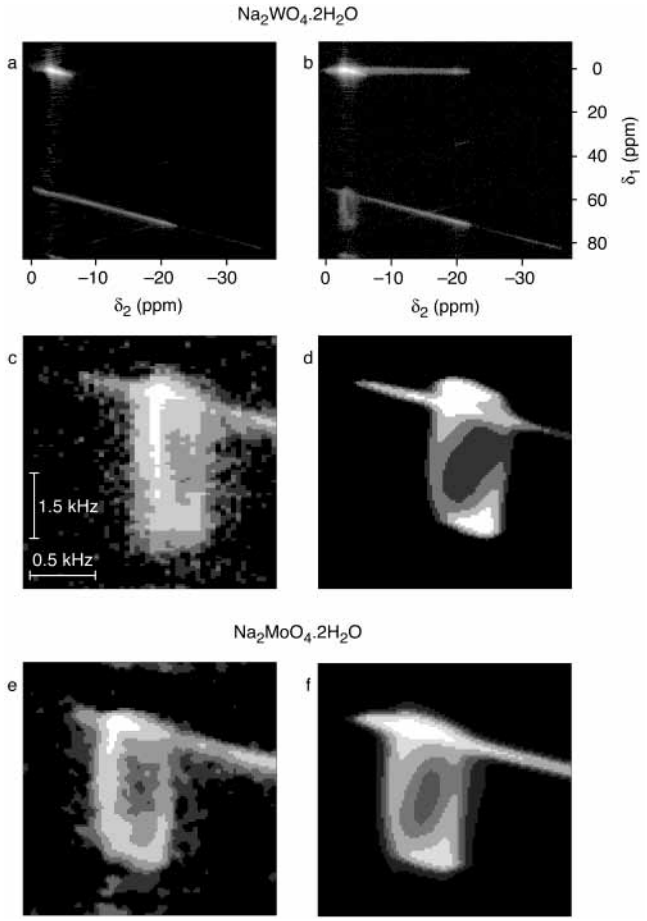

Figure 10. Experimental and computer-simulated two-dimensional triple-quantum ^{23}Na MAS NMR spectra of (a−d) sodium tungstate dihydrate ($Na_2WO_4 \cdot 2H_2O$) and (e, f) sodium molybdate dihydrate ($Na_2MoO_4 \cdot 2H_2O$). The cross-peak in (c) is an expansion of the low-field cross-peak in (b) and (d) is a simulation with relative tensor orientation (α', β', γ') = (90°, 24°, 15°). The cross-peak in (e) is an expansion of the corresponding cross-peak in the spectrum of $Na_2MoO_4 \cdot 2H_2O$ and (f) is a simulation with relative orientation as in (d). Experimental parameters in (a, b): pulse sequence in Figure 1b; (a) $\tau_m = 0$ and (b) $\tau_m = 200$ ms with no ^{1}H decoupling; 48 transients averaged for 512 t_1 increments of 16.67 μs; 3.0 s recycle interval; and 9.0 kHz MAS rate. Simulation parameters in (d): $C_{Q_1} = 0.88$ MHz; $C_{Q_2} = 2.70$ MHz; $\eta_1 = 0.35$; $\eta_2 = 0.09$; $\delta_{CS_1} = -0.9$ ppm; $\delta_{CS_2} = 6.3$ ppm; $\omega_0/2\pi = 105.8$ MHz; and 35 Hz Lorentzian linebroadening (full-width at half-height). Experimental parameters in (e): pulse sequence in Figure 1b; $\tau_m = 200$ ms with no ^{1}H decoupling; 24 transients averaged for 512 t_1 increments of 16.67 μs; 3.0 s recycle interval; and 9.0 kHz MAS rate. Simulation parameters in (f): $C_{Q_1} = 0.88$ MHz; $C_{Q_2} = 2.68$ MHz; $\eta_1 = 0.23$; $\eta_2 = 0.08$; $\delta_{CS_1} = -1.4$ ppm; $\delta_{CS_2} = 4.0$ ppm; $\omega_0/2\pi = 105.8$ MHz; and 35 Hz Lorentzian linebroadening (full-width at half-height).

of the molybdate ($C_{Q_1} = 0.88$ MHz, $C_{Q_2} = 2.68$ MHz, $\eta_1 = 0.23$, $\eta_2 = 0.08$, $\delta_{CS_1} = -1.4$ ppm, and $\delta_{CS_2} = 4.0$ ppm).[30] Figure 10d therefore shows the tungstate cross-peak simulated using the tungstate NMR parameters and a relative tensor orientation given by the Euler angles (α', β', γ') = (90°, 24°, 15°) found in our earlier molybdate study.[8] For comparison, the corresponding cross-peak from a triple-quantum MAS correlation spectrum of sodium molybdate dihydrate is shown in Figure 10e and its simulation in Figure 10f. Although all four cross-peaks expanded in Figure 10 show broad agreement, the experimental tungstate cross-peak in Figure 10c differs significantly from its simulation. Possible reasons for this difference include poor sample crystallinity[31] or motional effects.[32]

Conclusions

We have provided a detailed discussion of a novel two-dimensional MAS NMR technique that allows the relative orientation of quadrupole tensors to be determined from powdered crystalline solids. The use of a multiple-quantum approach offers an increase in resolution over conventional MAS techniques allowing accurate measurement of the Euler angles (α', β', γ') that describe the relative orientation. We have derived analytical expressions that permit simulation of the two-dimensional cross-peaks that arise in this experiment and have shown the sensitivity of the cross-peak shape to a change in any of the three Euler angles. We have demonstrated the utility of this method through ^{23}Na NMR of borax ($Na_2B_4O_7 \cdot 10H_2O$), sodium metasilicate pentahydrate ($Na_2SiO_3 \cdot 5H_2O$), sodium tungstate dihydrate ($Na_2WO_4 \cdot 2H_2O$), and sodium molybdate dihydrate ($Na_2MoO_4 \cdot 2H_2O$).

Acknowledgment. We are grateful to EPSRC for a studentship (N.G.D.) and for generous support (Grant GR/N07622).

Note Added after Publication. Due to a production error, Figure 4 was incomplete in this article, published on the Web 09/24/2002 (ASAP) and in the October 17, 2002, issue (Vol. 106, No. 41). The complete Figure 4 was replaced in the electronic version on 12/04/2002 and appears as an Addition and Correction in the December 26, 2002 issue (Vol. 106, No. 51).

References and Notes

(1) Abragam, A. *The Principles of Nuclear Magnetic Resonance*; Oxford University Press: Oxford, 1961.
(2) Andrew, E. R. In *Encylopedia of Nuclear Magnetic Resonance*; Grant, D. M., Harris, R. K., Eds.; Wiley: Chichester, 1996; p 2891.
(3) Ganapathy, S.; Schramm, S.; Oldfield, E. *J. Chem. Phys.* **1982**, *77*, 4360.
(4) Mueller, K. T.; Sun, B. Q.; Chingas, G. C.; Zwanziger, J. W.; Terao, T.; Pines, A. *J. Magn. Reson.* **1990**, *86*, 470.
(5) Samoson, A.; Lippmaa, E.; Pines, A. *Mol. Phys.* **1998**, *65*, 1013.
(6) Frydman, L.; Harwood, J. S. *J. Am. Chem. Soc.* **1995**, *117*, 5367.
(7) Gan, Z. *J. Chem. Phys.* **2001**, *114*, 10845.
(8) Dowell, N. G.; Ashbrook, S. E.; McManus, J.; Wimperis, S. *J. Am. Chem. Soc.* **2001**, *123*, 8135 [Correction: **2002**, *124*, 1125].
(9) Fernandez, C.; Amoureux, J. P. *Solid State Nucl. Magn. Reson.* **1996**, *5*, 315.
(10) Massiot, D.; Touzo, B.; Trumeau, D.; Coutures, J. P.; Virlet, J.; Florian, P.; Grandinetti, P. J. *Solid State Nucl. Magn. Reson.* **1996**, *6*, 73.
(11) Brown, S. P.; Wimperis, S. *J. Magn. Reson.* **1997**, *124*, 279.
(12) Brown, S. P.; Wimperis, S. *J. Magn. Reson.* **1997**, *128*, 42.
(13) Pike, K. J.; Malde, R. P.; Ashbrook, S. E.; McManus, J.; Wimperis, S. *Solid State Nucl. Magn. Reson.* **2000**, *16*, 203.
(14) Linder, M.; Höhener, A.; Ernst, R. R. *J. Chem. Phys.* **1980**, *73*, 4959.
(15) Shore, J. S.; Wang, S. H.; Taylor, R. E.; Bell, A. T.; Pines, A. *J. Chem. Phys.* **1996**, *105*, 9412.
(16) Jeener, J.; Meier, B. H.; Bachmann, P.; Ernst, R. R. *J. Chem. Phys.* **1979**, *71*, 4546.
(17) Ding, S. W.; McDowell, C. A. *Mol. Phys.* **1995**, *85*, 283.
(18) Cuthbert, J. D.; Petch, H. E. *J. Chem. Phys.* **1963**, *39*, 1247.
(19) Bloembergen, N.; Shapiro, S.; Pershan, P. S.; Artman, J. O. *Phys. Rev.* **1959**, *114*, 445.
(20) Meier, B. H. *Adv. Magn. Opt. Reson.* **1994**, *18*, 1.
(21) Baldus, M.; Rovnyak, D.; Griffin, R. G. *J. Chem. Phys.* **2000**, *112*, 5902.
(22) Nijman, M.; Ernst, M.; Kentgens, A. P. M.; Meier, B. H. *Mol. Phys.* **2000**, *98*, 161.
(23) Edén, M.; Frydman, L. *J. Chem. Phys.* **2001**, *114*, 4116.
(24) Bodenhausen, G.; Kogler, H.; Ernst, R. R. *J. Magn. Reson.* **1984**, *58*, 370.
(25) Amoureux, J. P.; Fernandez, C.; Steuernagel, S. *J. Magn. Reson. A* **1996**, *123*, 116.
(26) Amoureux, J. P. *Solid State Nucl. Magn. Reson.* **1993**, *2*, 83.
(27) Zare, R. N. *Angular Momentum*; Wiley: Chichester, 1996.
(28) Edmonds, A. R. *Angular Momentum in Quantum Mechanics*; Princeton University Press: Princeton, 1960.
(29) Koller, H.; Engelhardt, G.; Kentgens, A. P. M.; Sauer, J. *J. Phys. Chem.* **1994**, *98*, 1544.
(30) Skibsted, J.; Jakobsen, H. J. *Solid State Nucl. Magn. Reson.* **1994**, *3*, 29.
(31) Matsumoto, K.; Kobayashi, A.; Sasaki, Y. *Bull. Chem. Soc. Jpn.* **1975**, *48*, 1009.
(32) Schurko, R. W.; Wi, S.; Frydman, L. *J. Phys. Chem. A* **2002**, *106*, 51.